Journal of Applied Polymer Science

Preparation and Characterization of Polychloroprene Nanocomposites with Cellulose Nanofibers from Oil Palm Empty Fruit Bunches as a Nanofiller

Farah Fahma,[1,2] Naruhito Hori,[1] Tadahisa Iwata,[1] Akio Takemura[1]

[1]Department of Biomaterial Sciences, Graduate School of Agricultural and Life Sciences, University of Tokyo, 1-1-1 Yayoi, Bunkyo-Ku, Tokyo 113-8657, Japan

[2]Department of Agroindustrial Technology, Bogor Agricultural University, Kampus Institut Pertanian Bogor (IPB) Darmaga, Bogor, Indonesia

Correspondence to: A. Takemura (E-mail: akiot@mail.ecc.u-tokyo.ac.jp)

ABSTRACT: Cellulose nanofibers (CNFs) from oil palm empty fruit bunches were chemically modified by acetylation with acetic anhydride and pyridine (as the solvent and catalyst). The acetylated CNFs showed good dispersion in a polychloroprene (PCR) matrix. The tensile strength and modulus of neat PCR were improved, whereas its elongation at break decreased with increasing nanofiber content. Above the glass-transition temperature (T_g), the dynamic mechanical analysis profiles showed that the storage modulus of the PCR–cellulose nanocomposites was higher than that of neat PCR. Meanwhile, the thermal stability was still maintained, and the T_g was close to the neat PCR at the 5 wt % addition level of CNFs. © 2013 Wiley Periodicals, Inc. J. Appl. Polym. Sci. **2014**, *131*, 40159.

KEYWORDS: biomaterials; cellulose and other wood products; composites; elastomers; nanoparticles; nanowires and nanocrystals

Received 23 July 2013; accepted 2 November 2013

DOI: 10.1002/app.40159

INTRODUCTION

Recently, many publications are available that focus on composites reinforced with renewable materials including cellulose nanofibers (CNFs). Considering the hydrogen-bonding hydroxyl groups, CNFs have good potency as nanofillers in polar polymer matrixes.

Good dispersion of CNFs in the polymer matrix is a prerequisite for producing polymer–cellulose nanocomposites that exhibit a significant mechanical reinforcement. However, their high surface area and large hydrogen forces among themselves can lead to the formation of strongly bound aggregates and result in inefficient compounding with most nonpolar polymers.[1–3]

It was reported that besides in water, the CNFs also disperse well in solvents with medium polarity, such as *N*,*N*-dimethylacetamide and dimethylformamide; these solvents are very limited in terms of use.[4,5] Therefore, to extend the applications of CNFs as nanofillers in elastomer composites, the surface properties of the nanofibers should be modified to prevent self-aggregation and to improve dispersion and interfacial adhesion in the polymeric matrix by chemical modification of the surface. The main challenge in the chemical modification of CNFs is that the reaction process needs to be conducted in such a way that the intrinsic structure of the nanofibers, such as the original crystalline structure, is not destroyed.[6–8]

Polychloroprene (PCR) is an elastomer with rubberlike properties, including a low modulus, high elongation, and rapid recovery from deformation. PCR is a synthetic rubber with unique properties, such as ozone resistance, oil resistance, toughness, and heat resistance up to 100°C. This rubber has been commonly used as a material for hoses, roll covers, conveyor belts, air spring bellows, cables, sponge rubber, corrosion-resistant linings, sheeting, fabric proofing and footwear, power belts, boots, water suits and water sealant, and many medical support braces, such as those for ankles, wrists, and knees.[9,10]

In this study, the surface of CNFs was chemically modified by acetic anhydride to provide acetylated CNFs. The addition of a small amount of CNFs was expected to increase the properties of neat PCR. The nanofibers obtained from oil palm empty fruit bunches (OPEFBs) were used as a reinforcing filler to prepare the PCR nanocomposites. The acetylation dispersed the CNFs in dichloromethane, an organic solvent with a low polarity. Moreover, the acetylation reaction promoted the miscibility and interfacial adhesion of the nanofibers with the PCR matrix and ultimately enhanced the mechanical properties of the nanocomposites. Successful acetylation was confirmed by Fourier transform infrared (FTIR) spectroscopy. The PCR–acetylated cellulose nanocomposites were characterized with wide-angle X-ray diffraction (WAXD), tensile testing, dynamic mechanical analysis (DMA), thermogravimetric analysis (TGA), and differential scanning calorimetry (DSC).

EXPERIMENTAL

Materials

OPEFBs, supplied by PT Perkebunan Nusantara VIII Kertajaya (Lebak, Indonesia), were used to obtain the CNFs. Sulfuric acid (95%), acetone, dichloromethane, pyridine, acetic anhydride, and other chemicals, including ethanol, benzene, sodium chlorite, acetic acid, potassium hydroxide, and sodium hydroxide, were supplied by WAKO Pure Chemical Industries, Ltd. PCR was kindly supplied by Denki Kagaku Kogyo Kabushiki Kaisha (Japan).

Preparation of the CNFs

Cellulose fibers from OPEFBs were prepared as described in our previous work.[11,12] The cellulose fibers were hydrolyzed in a sulfuric acid solution (64 wt %) under strong agitation at 45°C for 60 min. Hydrolysis was terminated by the addition of cold water. The diluted suspension was centrifuged at 11,000 rpm for 10 min to obtain a precipitate. The precipitate was resuspended in water with strong agitation, followed by centrifugation. This process was repeated until the pH of the suspension reached more than 5. The suspension was dialyzed for 3 days until the pH became constant. Subsequently, the suspension was sonicated for 20 min to disperse the nanofibers in water with an ultrasonic homogenizer at a 200 W of output power (probe tip diameter = 26 mm, UD-201, Tomy Ultrasonic Disruptor, Japan).

Acetylation of the CNFs

Acetylation was performed as described in the literature.[8] Freeze-dried CNFs (1.0 mg) were dispersed in pyridine (70 mL). Chemical modification was started by the dropwise addition of acetic anhydride solution into the nanofiber suspension in pyridine. The reaction mixture was kept at 80°C under a nitrogen atmosphere and stirred for 5 h. The reaction was terminated through the addition of 1.0 L of water and washed several times with water. The solvent-exchange method was used to disperse the CNFs in dichloromethane. Sonication was performed after each solvent-exchange step to prevent aggregation.

PCR Nanocomposite Preparation

PCR–cellulose nanocomposites with 0, 1, 3, and 5 wt % nanofibers were prepared. The PCR solution in dichloromethane (10 wt %) and the acetylated nanofibers in dichloromethane were mixed and stirred for 10 min. Subsequently, the mixtures were cast in Teflon dishes and dried at room temperature for several days.

Characterization

Atomic Force Microscopy (AFM) Observation. The morphology of the CNFs dispersed in water was examined with an AFM scanning probe system composed of S-images, a Nano Navi II station, and an SI-AF-01 cantilever with Spisel32 AFM software (SII Nanotechnology, Inc., Japan). To prepare the sample, a drop of diluted nanofiber suspension (0.001 wt %) was placed onto freshly cleaved mica and dried at room temperature. Because of the possible agglomeration and broadening effect of the CNFs, only the thickness of the nanofibers was estimated by the measurement of the differences between the mica surface and nanofibers with the AFM software (Spisel32).[11] Fifty fibers in the AFM image for each sample were randomly selected, and the average diameters were calculated.

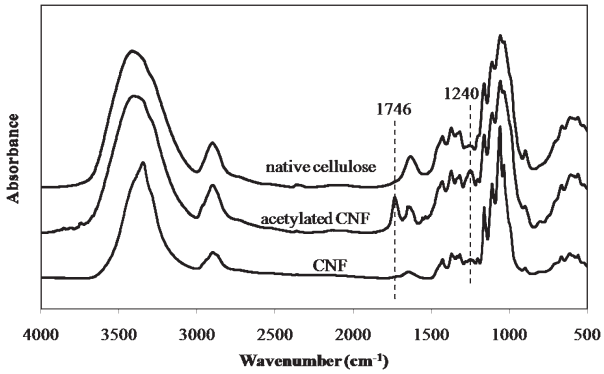

Figure 1. FTIR spectra of the native cellulose, CNFs, and acetylated nanofibers.

Scanning Electron Microscopy (SEM) Observation. The morphology of the unacetylated and acetylated nanofibers dispersed in dichloromethane was observed by SEM (JEOL S4800, Japan) operated at 10 kV. One droplet of suspension was placed on the surface of freshly cleaved mica and dried at room temperature. SEM was also used to evaluate the morphology of the neat PCR and its nanocomposites. Before analysis, the specimen was sputter-coated with platinum. From the SEM image, 50 fibers for each sample were randomly selected, and the average diameters were calculated.

X-ray Diffraction Analysis. The diffraction patterns of the neat PCR and its nanocomposites were obtained from radiation generated by the copper target of a Rigaku RINT2000 set at 38 kV and 50 mA with the detector placed on a goniometer that scanned from 5 to 35°. The degree of crystallinity was calculated from the diffraction profiles as the ratio of the area under the crystalline diffraction peaks to the total area under the curve.[13]

Tensile Test. The tensile tests for all samples were performed with an EZ Test machine (Shimadzu, Japan). We prepared the samples by cutting rectangular strips from the sheets with a width and length of 5 and 10 mm, respectively. Three specimens of each formulation were tested.

DMA. DMA of the neat PCR and its nanocomposites was performed with a DVA-200S analyzer. The specimens with dimensions of 30 × 5 × 0.3 mm^3 were scanned over a temperature range of −150 to +50°C. The frequency of the oscillations was fixed at 1 Hz, and the strain amplitude was 0.05%; this was well within the linear viscoelastic region. The heating rate was 1°C/min for all of the temperature scan tests.

TGA. TGA of the neat PCR and its nanocomposites was carried out with a Thermo Plus TG 8120 instrument. Thermograms were acquired between room temperature and 500°C at a heating rate of 10 K/min, with nitrogen as the purge gas at a flow rate of 110 mL/min. An empty pan was used as the reference.

DSC. DSC analysis of the neat PCR and its nanocomposites was performed on a Thermo Plus DSC 8230 at heating rate of 10 K/min under a nitrogen atmosphere. The thermograms were

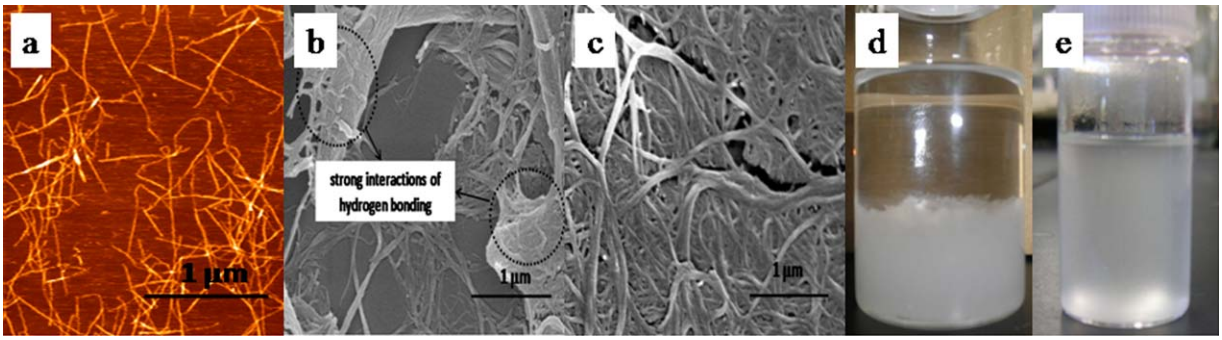

Figure 2. (a) AFM image of the CNFs from OPEFBs dispersed in water; (b,c) SEM images of unacetylated and acetylated nanofibers, respectively, dispersed in dichloromethane; and (d,e) photographs of unacetylated and acetylated nanofibers, respectively, dispersed in dichloromethane after 3 weeks. [Color figure can be viewed in the online issue, which is available at wileyonlinelibrary.com.]

acquired between −70 and 100°C. Approximately 4-mg samples were used for each analysis. The glass-transition temperature (T_g) was determined from the heating scan of the samples.

RESULTS AND DISCUSSION

Acetylation of the CNFs from the OPEFBs

Figure 1 shows the FTIR spectra of the native cellulose, acetylated nanofibers, and CNFs. After the acetylation reaction, a peak around 1746 cm^{-1}, assigned to the carbonyl C═O stretching of ester, appeared. A new absorption band at 1240 cm^{-1}, attributed to the C—O stretching of acetyl groups, also appeared. Meanwhile, the intensity of the peaks around 3344–3420 cm^{-1}, attributed to the O—H stretching of the CNFs, did not exhibit any trends. This might have been due to the very partial acetylation of the CNFs so that the acetylation process did not influence the hydrogen bonding of the CNFs.

AFM and SEM were used to investigate morphological changes of the CNFs associated with the surface acetylation. CNFs dispersed in water had an average thickness of around 3 ± 1.5 nm, as shown in the AFM image in Figure 2(a). Before acetylation, the CNFs were dispersed in pyridine. The pyridine was used as a solvent and a catalyst at same time. After acetylation with acetic anhydride, the acetylated nanofibers were dispersed in dichloromethane by a solvent-exchange method. It seemed that

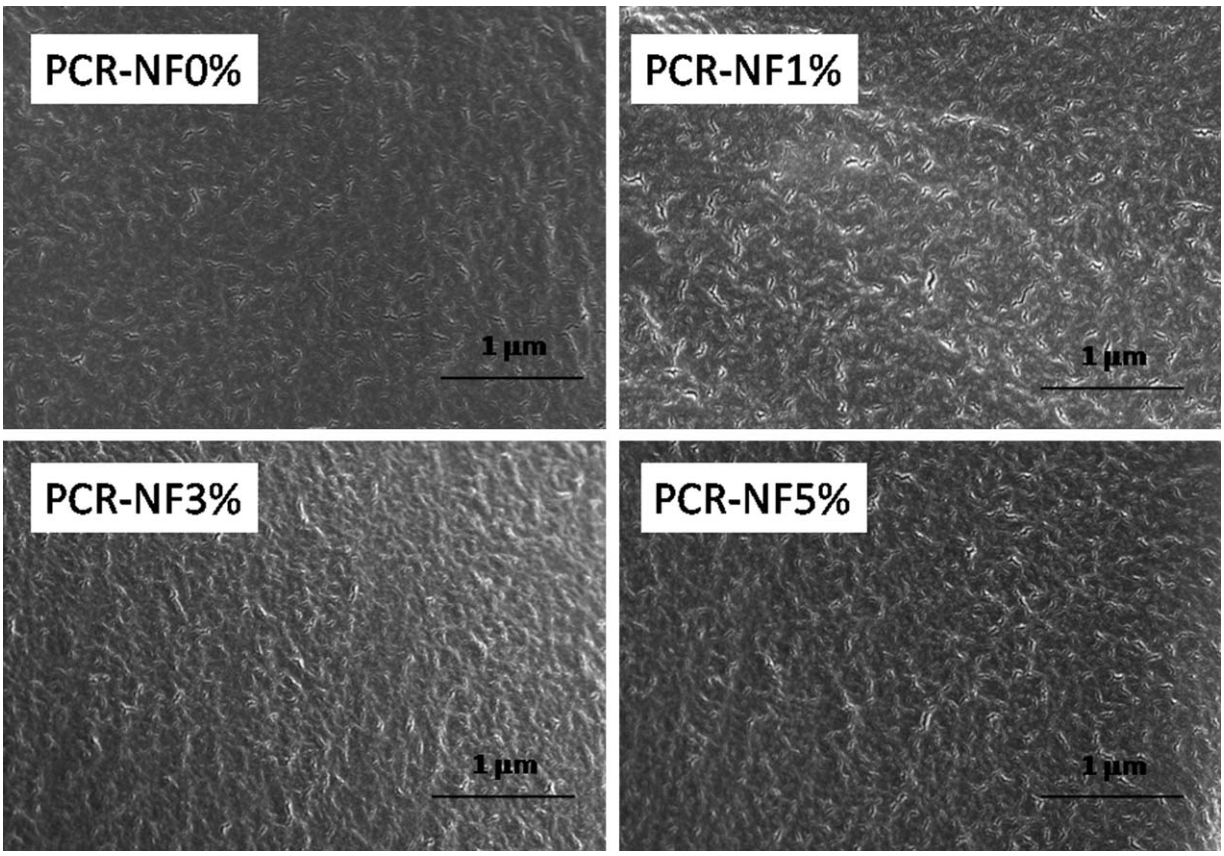

Figure 3. SEM images of the neat PCR and its nanocomposites.

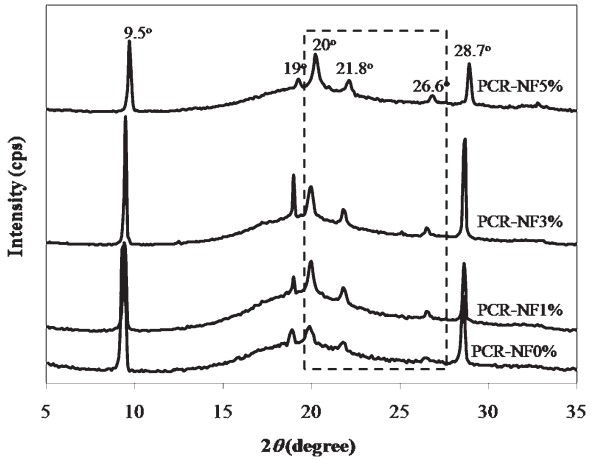

Figure 4. WAXD patterns of the neat PCR and its nanocomposites.

the nanofibers tended to aggregate to form bundles, as shown in the SEM image [Figure 2(c)]. The acetylated nanofibers had a diameter of 33 ± 14 nm.

The CNFs without surface modification had intrinsically strong interactions of hydrogen bonding so that they were difficult to disperse in nonpolar solvents [Figure 2(b,d)]. With these acetylation conditions, the nanofibers were easily dispersed in dichloromethane. The acetylated nanofibers suspensions showed good enough dispersion and stability in dichloromethane [Figure 2(e)]. The good enough dispersion of acetylated nanofibers in the dichloromethane as a solvent may have been due to the weakening of intramolecular and intermolecular hydrogen bonding due to the modification of the surface of the nanofibers.[8]

PCR–Cellulose Nanocomposites

The SEM images were used to compare the cross sections of all of the nanocomposites. Through SEM study, the distribution and compatibility between the CNFs as fillers and the PCR matrix were analyzed. Figure 3 shows that the addition of 1, 3, and 5% CNFs led them to mix well with the PCR matrix. All of the films indicated that the levels of interfacial bonding between the fibers and the matrix were similar to each other.

WAXD studies were performed to investigate whether any crystallinity in the nanocomposites changed with the increasing content of acetylated nanofibers. Figure 4 shows the X-ray diffraction patterns of the neat PCR and its nanocomposite sheets with different acetylated CNF content. There were six main peaks in all of the curves around 2θ values of 9.5, 19, 20, 21.8, 26.6, and 28.7°. The three peaks around 9.5, 19, and 28.7° were attributed to talc which had already been in PCR.[14] Therefore,

Table I. Degree of Crystallinity of the Neat PCR and Its Nanocomposites

Sample	Crystallinity (%)
PCR-NF0%	6.8 ± 0.7
PCR-NF1%	9.6 ± 0.5
PCR-NF3%	9.5 ± 0.6
PCR-NF5%	9.7 ± 0.4

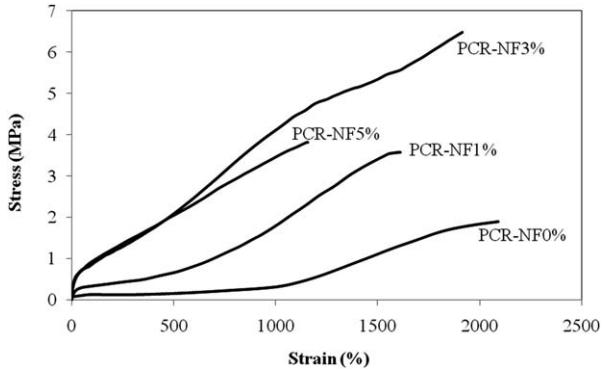

Figure 5. Typical stress–strain curves from the tensile tests for the neat PCR and its nanocomposites.

the crystallinities of the neat PCR and its nanocomposites were calculated from three other peaks (ca. 20, 21.8, and 26.6°). With the addition of the acetylated CNFs, the crystallinity of the PCR matrix increased (Table I).

The typical stress–strain curves of the neat PCR and its nanocomposites are shown in Figure 5. The values of the tensile strength, tensile modulus, and elongation at break are shown in Table II. We observed that the tensile strength of the PCR matrix increased with increasing CNFs content. Even the tensile strength of the nanocomposites with 5 wt % nanofibers was lower than those with 3 wt % nanofibers. The modulus increased with increasing nanofiber content up to 5 wt %. Meanwhile, the neat PCR showed the highest elongation at break. Among all of the nanocomposites, the nanocomposites with 3 wt % nanofibers showed the highest tensile strength and elongation at break. We noted that the addition of 3 wt % CNFs increased the tensile strength and tensile modulus significantly and could maintain an elongation at break close to that of the neat PCR.

The tensile strength of the nanocomposite film with 3 wt % nanofiber loading (PCR–NF3%) showed a 242% increase compared to the neat PCR, whereas the nanocomposite sheet with 5 wt % nanofibers showed a 105% increase compared to the neat PCR. The significant increase in the modulus with respect to the neat PCR was obtained as a function of the nanofiber content. The modulus of the nanocomposite with 3 wt % nanofibers increased from 1.0 to 7.1 MPa (610%), whereas with that of the nanocomposites with 5 wt % nanofibers increased to 8.0 MPa (700%). The increased tensile modulus may have been related to the increased stiffness of the nanocomposite sheets

Table II. Mechanical Properties of the Neat PCR and Its Nanocomposites

Sample	Tensile strength (MPa)	Tensile modulus (MPa)	Elongation at break (%)
PCR-NF0%	1.9 ± 0.2	1.0 ± 1.0	2088.1 ± 20.2
PCR-NF1%	3.6 ± 0.7	2.7 ± 0.6	1591.4 ± 15.7
PCR-NF3%	6.5 ± 0.8	7.1 ± 0.5	1912.1 ± 12.8
PCR-NF5%	3.9 ± 0.5	8.0 ± 0.9	1169.9 ± 16.3

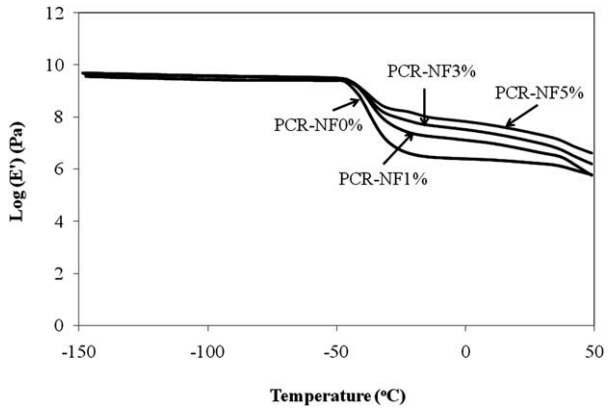

Figure 6. Log E' versus the temperature at 1 Hz for the neat PCR and its nanocomposites.

Table III. T_g and E' Values at −100 and 25°C

Sample	T_g (°C)	$E'_{-100°C}$ (GPa)	$E'_{25°C}$ (MPa)
PCR-NF0%	−49.1	2.7	1.7
PCR-NF1%	−47.1	3.7	5.2
PCR-NF3%	−46.1	3.9	12.2
PCR-NF5%	−46.0	3.8	25.2

with the addition of nanofibers because of the good enough dispersion of CNFs in the PCR matrix.

Figure 6 shows the logarithm of the storage modulus (E') at 1 Hz as a function of the temperature for the neat PCR and its nanocomposites. T_g can be determined from E'. Chen and Gardner[15] stated that from a mechanical point view, T_g determined from E' curves should be considered as it relates directly to the stiffness of the material. As shown in Figure 6, the T_g values of neat PCR and its nanocomposites with 1, 3, and 5 wt % of nanofibers was −49.5, −47, −46, and −46°C, respectively. The PCR nanocomposites exhibited a higher E' than the neat PCR above the T_g of rubber, as shown in Figure 6. Below T_g (−100°C), the E' values of all of the nanocomposites were almost similar each other,

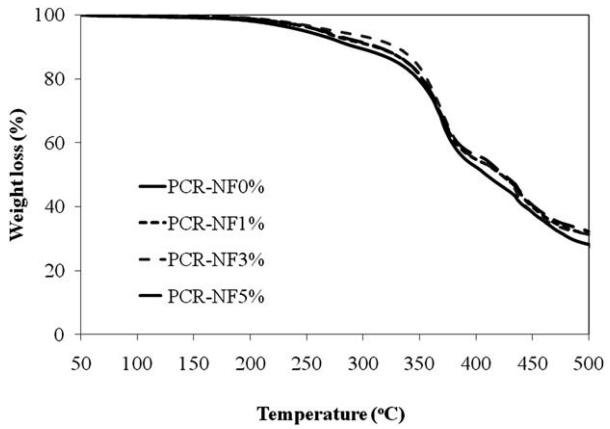

Figure 7. TGA curves of the neat PCR and its nanocomposites.

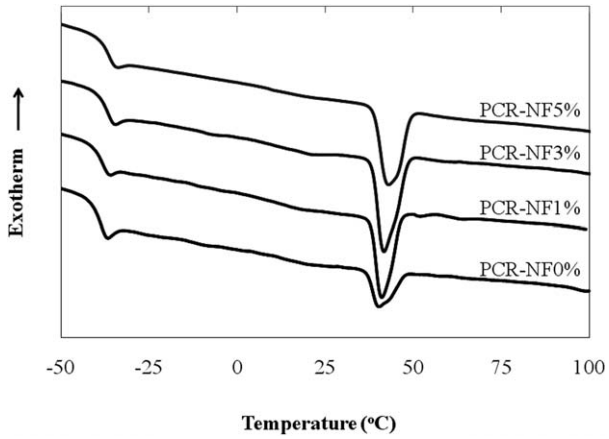

Figure 8. DSC curves of the neat PCR and its nanocomposites.

whereas the E' of neat PCR was 2.7 GPa. At room temperature (25°C), the E' of neat PCR dropped to 1.7 MPa. This value increased significantly with increasing nanofiber content. The addition of 5 wt % nanofibers improved the modulus of the neat PCR from 1.7 to 25.2 MPa (Table III).

An increase in the CNF content tended to increase E'. This might have been due to an increase in the entanglement between the nanofibers and the polymer matrix. Moreover, the strong interactions between the hydrogen bonds of CNFs caused the formation of a rigid network commanded by the percolation threshold.[16]

The thermogravimetric curves of the neat PCR and its nanocomposites containing different amounts of CNFs are shown in Figure 7. All of the curves obtained from the nitrogen environment showed a two-stage degradation process. Degradation started around 200°C. The first stage (primary decomposition) was dehydrochlorination, and it reached a maximum rate of weight loss around 366°C. The second stage was the decomposition of the residue, and it started around 400°C. Around 30% residue of the initial weight was left at 500°C.[17,18]

The DSC thermograms obtained for the neat PCR and its nanocomposites are shown in Figure 8. The thermal data obtained from the DSC curves are reported in Table IV. There was no significant difference in T_g for neat PCR and its nanocomposites. The T_g determined by the DSC measurements was lower than the T_g determined from the E' profiles.

As shown in Figures 7 and 8, with increasing CNF content, the degradation temperature and T_g values of the polymer matrix and its nanocomposites were close to each other. This was because the addition of CNFs within 5 wt % was still able to

Table IV. T_g, Melting Temperature (T_m), and Enthalpy of Melting (ΔH_m) for Neat PCR and Its Nanocomposites on the Basis of DSC Measurements

Sample	T_g (°C)	T_m (°C)	ΔH_m (J/g)
PCR-NF0%	−39.8	41.0	3.1
PCR-NF1%	−39.4	41.0	6.1
PCR-NF3%	−38.6	41.8	7.3
PCR-NF5%	−38.3	42.1	6.5

maintain the thermal stability of the polymer matrix. Moreover, the good dispersion of nanofibers in the polymer matrix might have still not been optimum because of the aggregation of some CNFs in the solvent.

CONCLUSIONS

Acetylated CNFs from OPEFBs exhibited a good dispersion in dichloromethane solvent. When 3 wt % acetylated CNF filler was introduced into the PCR matrix, the tensile strength of the PCR nanocomposite was enhanced by 242%, and the Young's modulus was seven-fold greater than that of the neat PCR sheet. This was mainly attributed to the good interfacial adhesion between the filler and the matrix. Moreover, the addition of acetylated CNFs maintained the thermal properties of the nanocomposites close to the neat PCR.

REFERENCES

1. Azizi Samir, M. A. S.; Alloin, F.; Sanchez, J. Y.; Dufresne, A. *Macromolecules* **2004**, *37*, 1386.
2. Azizi Samir, M. A. S.; Alloin, F.; Dufresne, A. *Biomacromolecules* **2005**, *6*, 612.
3. Azizi Samir, M. A. S.; Chazeau, L.; Alloin, F.; Cavaillé, J. Y.; Dufresne, A.; Sanchez, J. Y. *Electrochim. Acta* **2005**, *50*, 3897.
4. Tingaut, P.; Zimmermann, T.; Lopez-Suevos, F. *Biomacromolecules* **2010**, *11*, 454.
5. Fahma, F.; Hori, N.; Iwata, T.; Takemura, A. *J. Appl. Polym. Sci.* **2013**, *128*, 1563.
6. Dufresne, A. *J. Nanosci. Nanotechnol.* **2006**, *6*, 322.
7. Habibi, Y.; Lucia, A. L.; Rojas, O. *J. Chem. Rev.* **2010**, *110*, 3479.
8. Lin, N.; Huang, J.; Chang, P. R.; Feng, J.; Yu, J. *Carbohydr. Polym.* **2011**, *83*, 1834.
9. Das, A.; Mahaling, R. N.; Stöckelhuber, K. W.; Heinrich, G. *Compos. Sci. Technol.* **2011**, *71*, 276.
10. Lee, K. About Neoprene Fabric. http://www.ehow.com/about_4608813_neoprene-fabric.html. Accessed on 5 September 2011.
11. Fahma, F.; Iwamoto, S.; Hori, N.; Iwata, T.; Takemura, A. *Cellulose* **2010**, *17*, 977.
12. Fahma, F.; Iwamoto, S.; Hori, N.; Iwata, T.; Takemura, A. *Cellulose* **2011**, *18*, 443.
13. Wang, B.; Sain, M.; Oksman, K. *Appl. Compos. Mater.* **2007**, *14*, 89.
14. Riva, F.; Forte, A.; Della Monica, C. *Colloid Polym. Sci.* **1981**, *259*, 606.
15. Chen, J.; Gardner, D. *Polym. Compos.* **2008**, *29*, 372.
16. Favier, V.; Canova, G. R.; Cavaille, J. Y.; Chanzy, H.; Dufresne, A.; Gauthier, C. *Polym. Adv. Technol.* **1995**, *6*, 351.
17. Dick, C. M.; Liggat, J. J.; Snape, C. E. *Polym. Degrad. Stab.* **2001**, *74*, 397.
18. Gardner, D. L.; McNeill, I. C. *Eur. Polym. J.* **1971**, *7*, 569.